Gold-Catalyzed Direct Arylation

Liam T. Ball *et al.*

Science **337**, 1644 (2012);
DOI: 10.1126/science.1225709

voltage for a given current output) and 0.23%/°C (percentage change in resistance), both of which are consistent with the behavior of conventional, nontransient devices (*15*). Ultrathin Si solar cells (~3 μm thick) provide fill factors of 66% and overall power conversion efficiencies of ~3%, even without light-trapping structures, backside reflectors, or antireflection coatings. Doped Si NMs can serve as strain gauges (Fig. 3E, left), with gauge factors of nearly ~40 (Fig. 3F, left, and fig. S10B), which are comparable to those of state-of-the art devices (*16*). As an example of interconnected components, we built a transient digital imaging system, consisting of collections of Si NM photodiodes with blocking diodes for passive matrix addressing (Fig. 3E, right), capable of capturing pictures when operated in a scanned mode (Fig. 3F, right, and fig. S10D). (See more details on device dimensions in fig. S11.) The yield here is >90% [i.e., 58 out of 64 pixels were fully functional (fig. S12)]. One possibility for power supply involves Si solar cells such as those shown in fig. S10A. Another uses inductors and capacitors like those in Figs. 1A and 3A and fig. S9 as wireless antennas for near-field mutual inductance coupling to separately powered, external primary coils. This option is interesting for implantable devices (*4*), made possible by the biocompatibility of the constituent materials (Fig. 1), as established in unrelated contexts (*6*).

To demonstrate opportunities, we conducted a series of in vivo and in vitro experiments. Various representative transient devices were fabricated, sealed in silk packages, sterilized with ethylene oxide, and then implanted in the subdermal region of BALB/c mice in accordance with Institutional Animal Care and Use Committee protocols. Figure 4A shows the case of the platform in Fig. 1. Examination after 3 weeks (Fig. 4B, left) revealed only faint residues, with evidence of slow reintegration into the subdermal layers, along with apparent revascularization. The histological section in Fig. 4B (right) shows the subdermal layer (A), the silk film (B), and the muscle layer (C) and reveals no significant inflammatory reactions. Additional analysis appears in fig. S13.

Inductive coils of Mg combined with resistive microheaters of doped Si NMs, integrated on silk substrates and housed in silk packages, can provide transient thermal therapy to control surgical site infections (*17*, *18*) as a nonantibiotic, programmable bacteriocidal appliqué that disappears as the patient moves beyond the period of greatest risk. In vitro tests demonstrate the efficacy of this approach (*6*). Figure 4, C and D, present a metamaterial rf antenna, as a generalized component for such a device, capable of continuous wireless monitoring after implantation. The data indicate transient behavior associated with the slow diffusion of biofluids through the edges of the silk package, with a measured quality (Q) factor that has time dependence consistent with theoretical models (*6*). Figure 4E shows an image of a functional device formed on glass that includes two coils with different resonance frequencies (~70 and ~140 MHz) and three separate heaters. Wirelessly operating either or both of these coils with appropriate frequencies and power levels applied to a separate primary coil enables full control of the system, as illustrated in the thermal image in the inset. (See figs. S14 to S16 for other examples.) To illustrate in vivo functionality, a fully transient version of this device was implanted under the skin of a Sprague-Dawley rat (Fig. 4F). Inductive coupling through the skin generates a localized temperature increase of ΔT ~5°C (Fig. 4G), coincident with the position of the heater. The functional transience has a time scale of 15 days, chosen via the crystallinity of the silk, to coincide with the most critical period, which is the first few days after an operation, to sterilize and maintain asepsis at the wound site. After this time, the device disappears, leaving only remnants of silk, which resorb on longer time scales, to eliminate the long-term burden associated with additional exogenous implant material.

Concepts reported here establish a baseline of materials, modeling approaches, manufacturing schemes, and device designs for transient electronic systems, sensors, actuators, and power supplies. The Si NMs are critically important elements, because their use enables sophisticated semiconductor components with both active and passive functionality. For the dielectrics and conductors, additional possibilities range from collagen to poly(lactic-co-glycolic acid) and from iron to zinc, respectively. Alternative modes of transience include absorption, corrosion, and depolymerization. The rates for these processes could, conceivably, be adjustable in real time and/or sensitive to the properties of the surrounding environment, determined by chemical or biological events, or changes in temperature, pressure, or light. Combining such possibilities in transience with ideas in soft, tissue-like electronics will further expand opportunities for applications in biomedical devices (*7*).

References and Notes

1. C. J. Bettinger, Z. Bao, *Adv. Mater.* **22**, 651 (2010).
2. M. Irimia-Vladu *et al.*, *Adv. Funct. Mater.* **20**, 4069 (2010).
3. C. Legnani *et al.*, *Thin Solid Films* **517**, 1016 (2008).
4. D.-H. Kim *et al.*, *Nat. Mater.* **9**, 511 (2010).
5. Y. Wang *et al.*, *Biomaterials* **29**, 3415 (2008).
6. Information on materials and methods is available in the supplementary materials on *Science* Online.
7. D.-H. Kim *et al.*, *Science* **333**, 838 (2011).
8. R. K. Iler, *J. Colloid Interface Sci.* **43**, 399 (1973).
9. J. D. Rimstidt, H. L. Barnes, *Geochim. Cosmochim. Acta* **44**, 1683 (1980).
10. M. Morita, T. Ohmi, E. Hasegawa, M. Kawakami, M. Ohwada, *J. Appl. Phys.* **68**, 1272 (1990).
11. H. Seidel, L. Csepregi, A. Heuberger, H. Baumgartel, *J. Electrochem. Soc.* **137**, 3612 (1990).
12. R. D. Levine, *Molecular Reaction Dynamics* (Cambridge Univ. Press, Cambridge, 2005).
13. X. Hu *et al.*, *Biomacromolecules* **12**, 1686 (2011).
14. H.-J. Chung *et al.*, *Adv. Funct. Mater.* **21**, 3029 (2011).
15. S. Santra, P. K. Guha, S. Z. Ali, I. Haneef, F. Udrea, *IEEE Sens. J.* **10**, 997 (2010).
16. S. M. Won *et al.*, *IEEE Trans. Electron Devices* **58**, 4074 (2011).
17. *Am. J. Infect. Control* **24**, 380 (1996).
18. D. J. Anderson *et al.*, *PLoS ONE* **4**, 1 (2009); http://dx.doi.org/10.1371/journal.pone.0008305.

Acknowledgments: The work on materials, integration schemes, manufacturing approaches, and design strategies was supported by the Defense Advanced Research Projects Agency. The theoretical analysis and associated experiments were supported by an NSF INSPIRE grant. The techniques for creating and manipulating Si nanomembranes were developed in work supported by an Air Force Office of Scientific Research Multi University Research Initiative program. The animal studies were funded by the National Institutes of Health (grant EB002520). The facilities for characterization and analysis were provided by the Material Research Laboratory and Center for Microanalysis of Materials at the University of Illinois at Urbana–Champaign, both of which are supported by the U.S. Department of Energy.

Supplementary Materials

www.sciencemag.org/cgi/content/full/337/6102/1640/DC1
Materials and Methods
Figs. S1 to S22
References (*19*–*32*)

19 June 2012; accepted 29 August 2012
10.1126/science.1226325

Gold-Catalyzed Direct Arylation

Liam T. Ball, Guy C. Lloyd-Jones,* Christopher A. Russell*

Biaryls (two directly connected aromatic rings, Ar^1-Ar^2) are common motifs in pharmaceuticals, agrochemicals, and organic materials. Current methods for establishing the Ar^1-Ar^2 bond are dominated by the cross-coupling of aryl halides (Ar^1-X) with aryl metallics (Ar^2-M). We report that, in the presence of 1 to 2 mole percent of a gold catalyst and a mild oxidant, a wide range of arenes (Ar^1-H) undergo site-selective arylation by arylsilanes (Ar^2-$SiMe_3$) to generate biaryls (Ar^1-Ar^2), with little or no homocoupling (Ar^1-Ar^1/Ar^2-Ar^2). Catalysis proceeds at room temperature and tolerates a broad range of functional groups, including those incompatible with cross-coupling. These features expedite biaryl preparation, as demonstrated by synthesis of the nonsteroidal anti-inflammatory diflunisal.

The biaryl moiety (two directly connected aromatic rings, Ar^1-Ar^2) is a common functionality in pharmaceuticals [such as Lipitor, Crestor, and Diovan, three of the most widely prescribed drugs in 2010 (*1*)]; in agrochemicals; and in many modern organic materials, including liquid crystal displays, light-emitting diodes, and conducting polymers. The

high value of the biaryl motif is reflected in the myriad strategies for its construction, the majority of which involve transition metal–catalyzed cross-coupling of an aryl halide (Ar^1-X) and an aryl organometallic (Ar^2-M) (Fig. 1) (*2*, *3*). Nonetheless, it is widely appreciated that there remains a need for biaryl syntheses that are more concise, more selective, more versatile, or complementary to conventional routes. In response to this need, much effort has been devoted to direct arylation: cross-couplings in which one preactivated partner is replaced by a simple arene [for reviews, see (*4*–*7*); for selected examples, see (*8*–*14*)].

Direct arylation of an arene (Ar^1-H) with Ar^2-M constitutes coupling of two nominal nucleophiles and hence requires an oxidant. As a corollary of the oxidative mechanism, functional groups incompatible with traditional cross-coupling may be tolerated; for example, when one or both partners bear additional (pseudo)halogens (i.e., in Fig. 1, FG^1 and/or FG^2 = X^2, X^3). The mechanistically orthogonal direct arylation approach then facilitates a powerful synthetic strategy for step-economic construction of complex biaryl molecules; for example, delivering versatile halogenated biaryl systems primed for direct entry into the cross-coupling manifold. Although tremendous progress has been made in the field of (oxidative) direct arylation (*4*–*14*), delivery of an efficient protocol remains nontrivial. In particular, the inherent low reactivity of a C-H bond (relative to the C-X bond it replaces) must be overcome, and high selectivity must be exhibited for a specific C-H bond in Ar^1-H, without competition from C-H bonds in the coupling partner (Ar^2-M) or the product (Ar^1-Ar^2). Many of the extant methodologies involve harsh reaction conditions, limiting the substrate scope, and employ high catalyst loadings. Moreover, selectivity is frequently achieved by the use of an excess of one coupling partner (for example, as the solvent), and/or substrates incorporating a directing group capable of delivering the transition-metal catalyst to a specific C-H bond (*15*).

We report a gold-catalyzed direct arylation of simple arenes (Ar^1-H) with arylsilanes (Ar^2-$SiMe_3$) that affords biaryls (Ar^1-Ar^2) under remarkably mild conditions. The site of arylation is predictable and not dependent on the presence of adjacent, coordinating functionality. Both partners (Ar^1 and Ar^2) can be decorated with a diverse array of functionality, including halogens, thus providing valuable biaryl building blocks.

The stimulus for pursuing the direct arylation described here was provided by two recently disclosed gold-catalyzed processes: the dehydrogenative homocoupling of Ar^1-H in the presence of iodine(III), as reported by Tse (*16*, *17*), and a competing homocoupling of Ar^2-$SiMe_3$ that we observed in gold-catalyzed oxidative additions to alkenes (*18*, *19*). Although these reactions do generate biaryls, they are by definition symmetrical products (Ar^1-Ar^1 and Ar^2-Ar^2) and thus of limited value. Arylsilanes are well documented to react via electrophilic aromatic substitution pathways (S_EAr), analogously to simple arenes, with ipso substitution of the silyl moiety rather than loss of a proton (*20*). We thus hypothesized that S_EAr might be operative in both homocoupling processes. Extension of this argument raised the tantalizing possibility that site selective gold-catalyzed oxidative heterocoupling of arylsilanes with arenes (to give Ar^1-Ar^2) should provide a pathway for a synthetically valuable direct arylation. The feasibility of this process was confirmed by a ^{19}F nuclear magnetic resonance (NMR) study of mixtures of mesitylene (1,3,5-trimethylbenzene, Ar^1-H) with (4-fluorophenyl)trimethylsilane (Ar^2-$SiMe_3$) in the presence of a gold(I) precatalyst (Ph_3PAuCl) and an iodine(III) oxidant at 65°C. The desired direct arylation process was detected but accompanied by homocoupling of the arylsilane (Ar^2-Ar^2), a competing electrophilic substitution of Ar^1-H by iodine(III), and further arylation of the biaryl product (Ar^2-Ar^1-Ar^2).

Four criteria were identified as key for the delivery of a practical and general direct arylation process, leading us to engage in an extensive program of reaction refinement (*21*): (i) high selectivity for heterocoupling over homocoupling; (ii) economic, ideally stoichiometric, quantities of the reactants; (iii) tolerance of a wide range of functionalities; and (iv) efficient catalysis at convenient temperatures, without the need for inert atmospheres.

Using these criteria as guiding principles, conditions were developed that facilitate high-yielding direct arylation, in the majority of cases with near-complete suppression of all side reactions (Tables 1 and 2). Key developments were using $Ph_3PAuOTs$ as a precatalyst (table S2), conducting the reaction in the presence of a low concentration of methanol co-solvent at room temperature (tables S3 and S4), and forming the active oxidant in situ from iodobenzene diacetate [$PhI(OAc)_2$] and camphorsulfonic acid (CSA) (tables S1 and S4); the latter are both commercially available, bench-stable free-flowing solids. Control reactions established the essential role of a gold precatalyst over other late transition elements or Brønsted/Lewis acid promoters (table S5) and demonstrated both the innocence of diaryliodonium salt side-products and the absence of uncatalyzed arylation, even at elevated temperatures (schemes S1 and S2).

Two general sets of conditions were identified, which were tailored to the cost and complexity of the arene: for heavily functionalized or valuable arenes, a 1:1 stoichiometry of coupling partners was used (conditions **A**), whereas for simple or cheap arenes, a 2:1 stoichiometry was used and the precatalyst loading reduced from 2 to 1 mole % (mol %) (conditions **B**). Most reactions proceeded to completion within 20 to 40 hours at room temperature, although some were notably quicker (*21*). Longer reaction times (up to 80 hours) or higher temperatures (up to 65°C) were required when reactants were sterically hindered (**14**, **31**, and **32**), or when less electron-rich arenes (**4**, **8**, **20**, and **28**) or electron-deficient arylsilanes (**46** and **47**) were coupled, these reactivity trends being consistent with S_EAr elementary steps for both partners. The arylation process exhibits excellent site selectivity with respect to the arene partner (Ar^1-H, Table 1), the position of arylation also being readily predictable based on the well-understood patterns of S_EAr (*20*). The mildness of the conditions is evident from the

School of Chemistry, University of Bristol, Cantock's Close, Bristol BS8 1TS, UK.

*To whom correspondence should be addressed. E-mail: guy.lloyd-jones@bris.ac.uk (G.C.L.-J.); chris.russell@bris.ac.uk (C.A.R.)

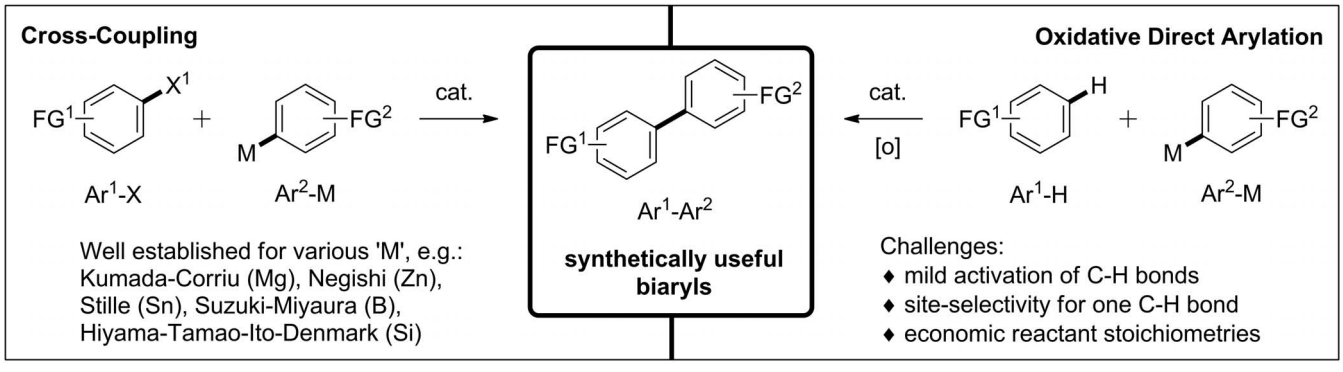

Fig. 1. Cross-coupling and oxidative direct arylation approaches to biaryl (Ar^1-Ar^2) building blocks. X^1, halide or sulfonate; M, electropositive element (such as Mg, Zn, B, Sn, or Si); $FG^{1\text{-}2}$, functional group (including alkyl, aryl, halogen etc); [O], oxidant; cat., transition-metal catalyst.

Table 1. Scope of Ar^1-H in Au-catalyzed direct arylation. Conditions: arylsilane (0.50 mmol), $PhI(OAc)_2$ (0.65 mmol), and CSA (0.75 mmol) in $CHCl_3/CH_3OH$ (50:1) at room temperature, and **A**, Ar^1-H (0.50 mmol) and $Ph_3PAuOTs$ (2 mol %); or **B**, Ar^1-H (1.00 mmol) and $Ph_3PAuOTs$ (1 mol %). Ts, *p*-toluenesulfonyl; Ms, methanesulfonyl; Piv, pivaloyl ($COCMe_3$); NPhth, *N*-phthalimido.

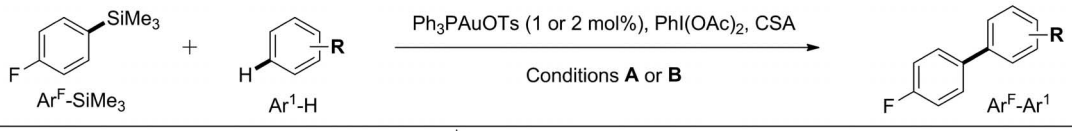

Conditions A.

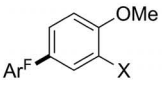

1 X = Cl 85%
2 X = Br 92%
3 X = I 88%
4 X = OMs 81% *
5 X = CO_2Me 92%
6 X = NMePiv 94%
7 X = NPhth 88%

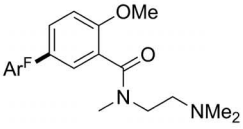

8 65% †, ‡

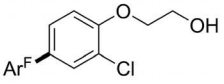

9 59% §

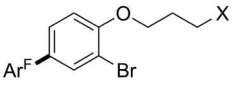

10 X = OH 82% ||
11 X = OMs 71%
12 X = $OCONiPr_2$ 69%
13 X = NPhth 83%

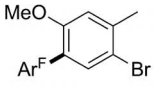

14 74%

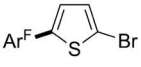

15 91%

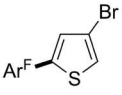

16 29% ¶

Conditions B.

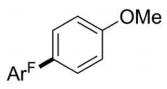

17 68% #

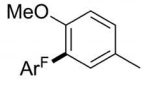

18 63% **

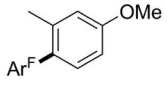

19 46% ††

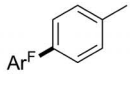

20 93% ‡‡

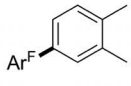

21 82% §§

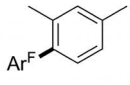

22 71%

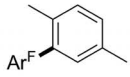

23 74%

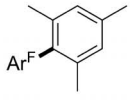

24 74%

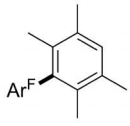

25 65%

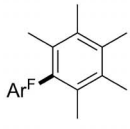

26 78% *

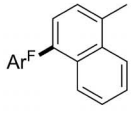

27 57% ||||

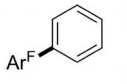

28 37% †, ¶¶

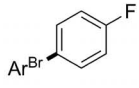

29 6% †, ‡, ##

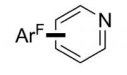

30 0 †

*0.75 mmol Ar^1-H. †IBA (1-hydroxy-1,2-benziodoxol-3-(1*H*)-one) replaces $PhI(OAc)_2$ at 65°C. ‡Yield by $^1H/^{19}F$ NMR. §1.5 mol % Au. ||With X = $OSiiPr_3$, in situ deprotection yields **10** (63%). ¶Site selectivity: 57%, with 2,5-diarylated thiophene (17%) also formed. #Site selectivity: 89%. **2,6-Diarylated anisole (10%) also formed. ††Site selectivity: 67%, with diarylated anisole also detected (8%, by gas chromatography–mass spectrometry). ‡‡Site selectivity: 80%. §§Site selectivity: 87%. || ||0.50 mmol Ar^1-H. ¶¶4,4′-Difluorobiphenyl (homocoupling product, 37%) and 1,4-diarylated benzene (10%) also formed. ##4-(Bromophenyl)trimethylsilane replaces 4-(fluorophenyl)trimethylsilane, Ar^{Br} = 4-bromophenyl.

reaction of (4-fluorophenyl)trimethylsilane with a range of ortho-anisole derivatives under conditions **A**, to give the corresponding biaryls in high yield and with excellent site selectivity (97 to 99% isomeric purity) (*21*).

A wide range of functional groups is tolerated, including synthetically useful (pseudo)halogenated species (**1** to **4**), esters and amides (**5** to **8**), and sensitive functionalities remote from the ring, such as primary alcohols (**9** and **10**) and sulfonate (**11**). Biaryl **8** also demonstrates tolerance of an amine in the gold-catalyzed direct arylation; a basic nitrogen moiety is present in all of the 10 most widely prescribed drugs of 2010 (*1*). In compounds **1** to **8**, **14**, and **17** to **19**, the methoxy substituent itself is of further synthetic potential; for example, directing S_EAr and ortho-metallation, or via derivatization, cross-coupling, amination, or reductive cleavage [for a review of catalytic activation of arylmethyl ethers, see (*22*)].

Simple arenes, including those lacking strongly electronically activating and/or directing groups, also proved excellent substrates and were ideal for reaction under conditions **B**; the site selectivity observed with anisole and toluene, giving biaryls **17** and **20**, respectively, being consistent with S_EAr by a gold(III) electrophile (*23*). Although the electron-rich 4-methylanisole, in which the position para to the methoxy substituent is blocked, promoted double arylation, **18** was generated with >99.7% discrimination between electronically different sites. In contrast, 3-methylanisole, in which the 4- and 6- positions are similarly activated, underwent arylation to give **19** as a 2:1 mixture of isomers. Arylation even occurred smoothly at C-H bonds flanked on either side by methyl substituents (**24** to **26**), and although the parent naphthalene reacted with low selectivity (*21*), the methyl-substituted analog generated biaryl **27** with >96% site selectivity, in just 5 hours at room temperature.

A preliminary investigation indicated that thiophenes are viable substrates, although, without further optimization, the conditions proved less general [for example, compare **15** (91%, >99.5% site selective) and **16** (29%, 57% site selective)]. The low reactivity of electron-deficient (hetero) arenes, such as PhF (**29**) and pyridine (**30**), is

Table 2. Scope of Ar^2-$SiMe_3$ in Au-catalyzed direct arylation. Reaction conditions are as in Table 1. Tf, trifluoromethanesulfonyl.

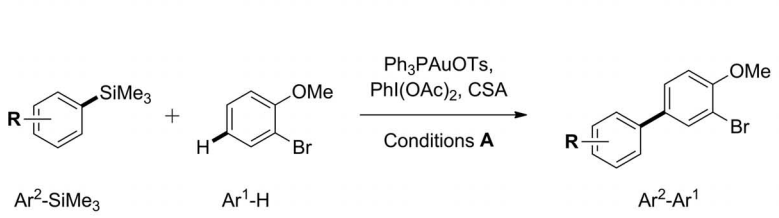

31	R = 2-F	92% *	**39**	R = 4-CO_2Me	70%
32	R = 2-OMs	70% *	**40**	R = 4-OTf	72% †
33	R = 4-Cl	97%	**41**	R = 4-OPiv	80%
34	R = 4-Br	91%	**42**	R = 4-NMePiv	59% ‡, §
35	R = 4-I	67%	**43**	R = 4-NMeTs	91%
36	R = 3-Br	72%	**44**	R = H	84% ‡
37	R = 3-CHO	77%	**45**	R = 4-Me	55% *, ‖
38	R = 4-Piv	90%			

*IBA replaces $PhI(OAc)_2$ at 65°C. †1 mol % Au. ‡Using conditions **B**. §Arylsilane homocoupling product (29%) also formed. ‖1.00 mmol Ar^1-H, arylsilane homocoupling product (23%) also formed.

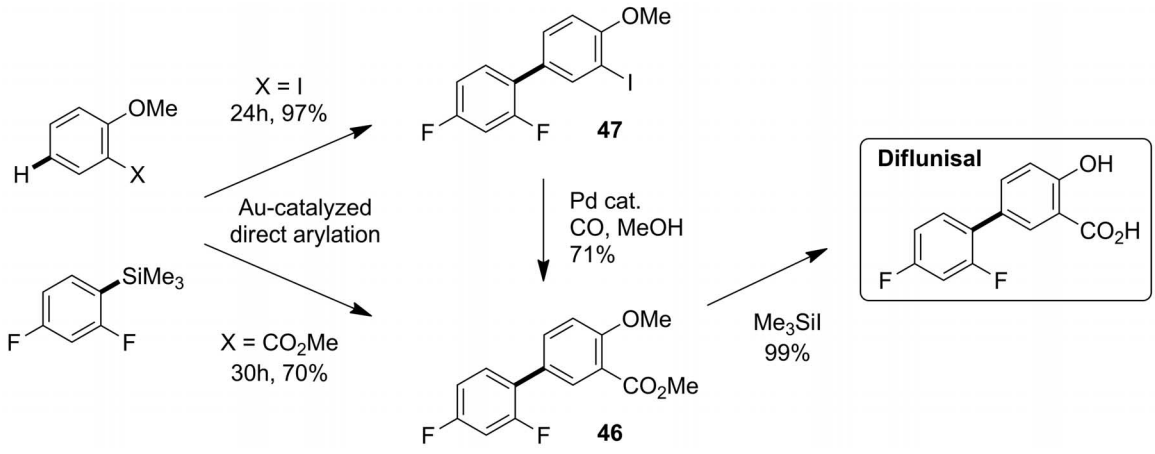

Fig. 2. Diflunisal via gold-catalyzed direct arylation; yields are unoptimized. Site selectivity for the arylation step (**46** and **47**) is 98 to 99%.

again consistent with an S_EAr mechanism. The selectivity for electron-rich aromatics not only suppresses over-arylation but is also complementary to direct arylation processes that proceed via deprotonation-type mechanisms and favor electron-poor substrates or require ortho-directing groups (*4*–*7*, *15*).

Diverse functionality could also be introduced through the arylating partner (Ar^2-$SiMe_3$, Table 2). Ortho-substituted arylsilanes that reacted sluggishly at room temperature gave the corresponding biaryls (e.g., **31** and **32**) in excellent yield at 65°C, using a less reactive iodine(III) oxidant. The synthetically useful halogens and sulfonates (**31** to **36** and **40**) were well tolerated, as were an aldehyde (**37**) and a pivaloyl ester (**41**) that remained in the products without oxidation or transesterification, respectively. Although electron-rich silanes proved more challenging, as a result of arylsilane homocoupling, the selection of appropriate reaction conditions allowed even biaryl **45** to be isolated in reasonable yield. Homocoupling of the arene partner (*16*, *17*) was not observed; instead, the material balance of the less efficient reactions detailed in Table 1 (typically for electron-rich Ar^1-H) comprised diarylation and diaryliodonium side products (*21*).

The utility of the direct arylation methodology is exemplified by the preparation of diflunisal (Dolobid, Merck & Co.), a non-opioid, nonsteroidal anti-inflammatory drug (*24*, *25*). Unoptimized direct arylation of methyl ortho-anisate (X = CO_2Me, Fig. 2) with (2,4-difluorophenyl)trimethylsilane afforded the corresponding biaryl **46**; routine demethylation gave diflunisal (69%). Previous methods for forging the key biaryl linkage of diflunisal include Gomberg-Bachmann coupling of a diazonium salt and traditional cross-coupling (*21*). The power of the direct arylation approach is also evident in a second route to diflunisal, proceeding via biaryl **47**; this iodide intermediate can also serve as a versatile platform for structural diversification via a broad spectrum of stoichiometric and catalytic methodologies, including cross-coupling.

Compared to many other direct arylations (*4*–*14*), gold-catalyzed arylation with arylsilanes is notable for its mild conditions, low loadings, and site selectivity. It also provides complementarity and orthogonality to traditional cross-coupling strategies (*2*, *3*), allowing the strategic linking of the two processes (Fig. 2). Arylsilanes are particularly valuable as substrates, because the stability of the silyl moiety allows it to be installed early in a synthesis, and they are readily handled, lacking the toxicity and/or air sensitivity that can be displayed by the aryl metallics traditionally used in cross-coupling. Their synthesis, via silylation of a range of precursors that includes arenes, aryl halides, benzonitriles, and arylmetallics, is generally straightforward (*21*), and both camphorsulfonic acid and iodobenzene diacetate are commercially available; alternatively, the latter can be very efficiently prepared from iodobenzene with a cheap stoichiometric oxidant (*21*). In addition, and in contrast to such metals as palladium and nickel, gold residues are regarded as relatively benign, and the $Ph_3PAuOTs$ precatalyst can be prepared in near-quantitative yield (*26*) in a single step from commercially available precursors. All of these aspects suggest the expedient application of gold-catalyzed direct arylation for the concise construction of synthetically valuable biaryl building blocks for pharmaceutical, agrochemical, and materials chemistry.

References and Notes

1. DrugTopics, http://drugtopics.modernmedicine.com/drugtopics/data/articlestandard//drugtopics/252011/727256/article.pdf; accessed 30 May 2012.
2. J. Tsuji, *Palladium Reagents and Catalysis: New Perspectives for the 21st Century* (Wiley, Chichester, UK, 2004).
3. C. C. C. Johansson Seechurn, M. O. Kitching, T. J. Colacot, V. Snieckus, *Angew. Chem. Int. Ed.* **51**, 5062 (2012).
4. L. Ackermann, R. Vicente, A. R. Kapdi, *Angew. Chem. Int. Ed.* **48**, 9792 (2009).
5. D. Alberico, M. E. Scott, M. Lautens, *Chem. Rev.* **107**, 174 (2007).
6. G. P. McGlacken, L. M. Bateman, *Chem. Soc. Rev.* **38**, 2447 (2009).
7. T. W. Lyons, M. S. Sanford, *Chem. Rev.* **110**, 1147 (2010).
8. M. Lafrance, K. Fagnou, *J. Am. Chem. Soc.* **128**, 16496 (2006).
9. S.-D. Yang *et al.*, *Angew. Chem. Int. Ed.* **47**, 1473 (2008).
10. J. Wen, J. Zhang, S.-Y. Chen, J. Li, X.-Q. Yu, *Angew. Chem. Int. Ed.* **47**, 8897 (2008).
11. R. J. Phipps, M. J. Gaunt, *Science* **323**, 1593 (2009).

12. H. Hachiya, K. Hirano, T. Satoh, M. Miura, *Angew. Chem. Int. Ed.* **49**, 2202 (2010).
13. C.-L. Ciana, R. J. Phipps, J. R. Brandt, F.-M. Meyer, M. J. Gaunt, *Angew. Chem. Int. Ed.* **50**, 458 (2011).
14. K. Funaki, H. Kawai, T. Sato, S. Oi, *Chem. Lett.* **40**, 1050 (2011).
15. S. R. Neufeldt, M. S. Sanford, *Acc. Chem. Res.* **45**, 936 (2012).
16. A. Kar, N. Mangu, H. M. Kaiser, M. Beller, M. K. Tse, *Chem. Commun.* 386 (2008).
17. A. Kar, N. Mangu, H. M. Kaiser, M. K. Tse, *J. Organomet. Chem.* **694**, 524 (2009).
18. L. T. Ball, M. Green, G. C. Lloyd-Jones, C. A. Russell, *Org. Lett.* **12**, 4724 (2010).
19. L. T. Ball, G. C. Lloyd-Jones, C. A. Russell, *Chemistry* **18**, 2931 (2012).
20. R. Taylor, *Electrophilic Aromatic Substitution* (Wiley, Chichester, UK, 1990).
21. See supplementary materials on *Science* Online for detailed methods and discussion.
22. B.-J. Li, D.-G. Yu, C.-L. Sun, Z.-J. Shi, *Chemistry* **17**, 1728 (2011).
23. R. O. C. Norman, W. J. E. Parr, C. B. Thomas, *J. Chem. Soc. Perkin Trans.* **1**, 1983 (1976).
24. W. V. Ruyle, L. H. Sarett, A. R. Matzuk, U.S. Patent 3,714,226 (1973).
25. J. Hannah *et al.*, *J. Med. Chem.* **21**, 1093 (1978).
26. P. Römbke, A. Schier, H. Schmidbaur, *J. Chem. Soc. Dalton Trans.* 2482 (2001).

Acknowledgments: Experimental procedures and compound characterization data are both presented in the supplementary materials. L.T.B., G.C.L.-J., and C.A.R contributed equally to the conception and direction of this work and to the preparation of the manuscript. L.T.B. conducted all of the experimental work. We thank Umicore AG & Co. KG for the generous donation of $HAuCl_4$. L.T.B. thanks the Bristol Chemical Synthesis Doctoral Training Centre, funded by the Engineering and Physical Sciences Research Council (grant EP/G036764/1); AstraZeneca; GlaxoSmithKline; Novartis; Pfizer; Syngenta; and the University of Bristol, for the provision of a Ph.D. studentship. G.C.L.-J. is a Royal Society Wolfson Research Merit Award holder.

Supplementary Materials
www.sciencemag.org/cgi/content/full/337/6102/1644/DC1
Materials and Methods
Supplementary Text
Figs. S1 and S2
Tables S1 to S5
Schemes S1 and S2
References (*27*–*101*)

6 June 2012; accepted 16 August 2012
10.1126/science.1225709

Synthesis and Characterization of a Rhodium(I) σ-Alkane Complex in the Solid State

Sebastian D. Pike,[1] Amber L. Thompson,[1] Andrés G. Algarra,[2] David C. Apperley,[3] Stuart A. Macgregor,[2]* Andrew S. Weller[1]*

Transition metal–alkane complexes—termed σ-complexes because the alkane donates electron density to the metal from a σ-symmetry carbon–hydrogen (C–H) orbital—are key intermediates in catalytic C–H activation processes, yet these complexes remain tantalizingly elusive to characterization in the solid state by single-crystal x-ray diffraction techniques. Here, we report an approach to the synthesis and characterization of transition metal–alkane complexes in the solid state by a simple gas-solid reaction to produce an alkane σ-complex directly. This strategy enables the structural determination, by x-ray diffraction, of an alkane (norbornane) σ-bound to a d^8–rhodium(I) metal center, in which the chelating alkane ligand is coordinated to the pseudosquare planar metal center through two σ-C–H bonds.

The recognition that the σ-bond of dihydrogen, or the C–H bond of an ancillary ligand (an intramolecular agostic interaction), can interact with a metal center to form a so-called σ-complex was a landmark discovery in transition metal chemistry (*1*). In such complexes, the C–H (or H–H) bonds serve as ligands to the metal center through donation of their σ-bonding electron pair. The chemistry of such species is now well established. In contrast, the synthesis of transition metal–alkane σ-complexes (Fig. 1) (*1*–*3*), key intermediates in C–H activation processes (*4*–*6*), represents one of the major challenges for organometallic chemists over the past 40 years. Although the first examples were suggested by spectroscopic data arising from matrix isolation experiments at 12 K (*7*), σ-complexes remain tantalizingly elusive species to characterize fully, especially compared with the closely related σ-complexes of H_2 (*1*) or agostic complexes (*8*). The existence of σ-complexes as intermediates is often inferred from detailed kinetic studies of C–H activation processes (*9*), whereas direct observation relies on solution spectroscopic techniques such as fast time-resolved infrared spectroscopy (*10*, *11*) or nuclear magnetic resonance (NMR) spectroscopy (*12*), generally at low temperatures (for example, at –83°C). Important recent advances include characterization of relatively long-lived (in hours) σ-alkane complexes in solution for a variety of simple alkanes using Mn- or Re-based metal fragments (*13*, *14*), as well as a methane σ-complex at a d^8–rhodium(I) center (Fig. 1A) (*15*). This complex, stable in $CDCl_2F$ solution at –110°C, is formed directly by protonation of a Rh–CH_3 bond.

Only two examples have been reported in which a saturated hydrocarbon has been located within the coordination sphere of a metal center in the solid state, allowing for an analysis of the molecular structure by single-crystal x-ray diffraction techniques. The first of these (Fig. 1B) shows a molecule of heptane interacting with an iron(II)–porphyrin complex (*16*). Unfortunately, crystallographic disorder prevented the accurate analysis of the Fe-alkane interaction. The second example (Fig. 1C) involves cyclic alkane adducts of an unsaturated uranium(III) complex (*17*). Both structures in Fig. 1, B and C, result from incorporation of a solvent molecule within the coordination sphere of the metal, potentially assisted by host-guest effects in addition to the direct C–H···M bond interaction (here, M represents a metal). Neither of these complexes are stable on solvation. Very recently, the binding of light alkanes to iron centers in an extended metal-organic framework was characterized by powder

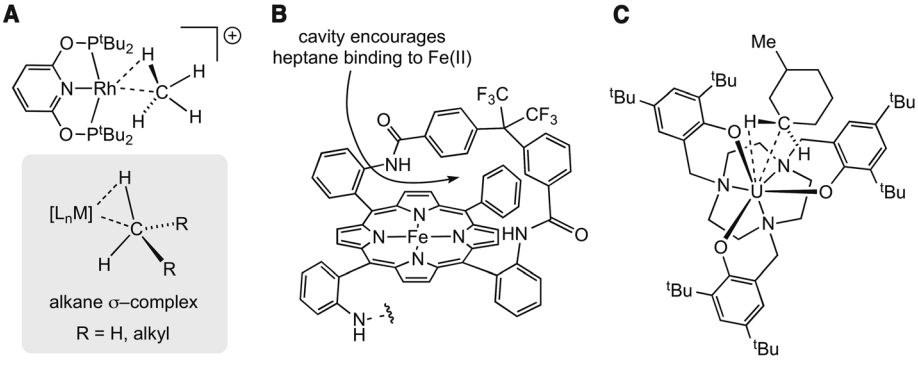

Fig. 1. Previously characterized σ-complexes in solution (**A**) and the solid state (**B** and **C**). L_n, ligands; ^{t}Bu, tertbutyl group; Me, methyl.

[1]Department of Chemistry, Chemical Research Laboratories, Mansfield Road, Oxford OX1 3TA, UK. [2]Institute of Chemical Sciences, Heriot-Watt University, Edinburgh EH14 4S, UK. [3]Engineering and Physical Sciences Research Council (EPSRC) Solid-State Nuclear Magnetic Resonance Service, Department of Chemistry, Durham University, South Road, Durham DH1 3LE, UK.

*To whom correspondence should be addressed. E-mail: andrew.weller@chem.ox.ac.uk (A.S.W.); s.a.macgregor@hw.ac.uk (S.A.M.)